Supplement of

Measurement report: The effect of aerosol chemical composition on light scattering due to the hygroscopic swelling effect

Rongmin Ren[1], Zhanqing Li[2], Peng Yan[3], Yuying Wang[4], Hao Wu[5], Wei Wang[1], Xiao'ai Jin[1], Yanan Li[3], Dongmei Zhang[1] and Maureen Cribb[2]

[1]State Key Laboratory of Remote Sensing Science, College of Global Change and Earth System Science, Beijing Normal University, Beijing 100875, China
[2]Earth System Science Interdisciplinary Center, Department of Atmospheric and Oceanic Science, University of Maryland, College Park, College Park, MD, USA
[3]CMA Meteorological Observation Center, Centre for Atmosphere Watch and Services, Beijing 100081, China
[4]Key Laboratory for Aerosol-Cloud-Precipitation of China Meteorological Administration, School of Atmospheric Physics, Nanjing University of Information Science and Technology, Nanjing 210044, China
[5]School of Electrical Engineering, Chengdu University of Information Technology, Chengdu 610225, China

Correspondence to: Zhanqing Li (zli@atmos.umd.edu)

The scattering and back-scattering coefficients at three wavelengths measured by the two nephelometers are highly consistent (Fig. S1). The slopes of the linear fittings are close to 1, and the coefficient of determination (R^2) is also close to 1, indicating that the two nephelometers are of good consistency.

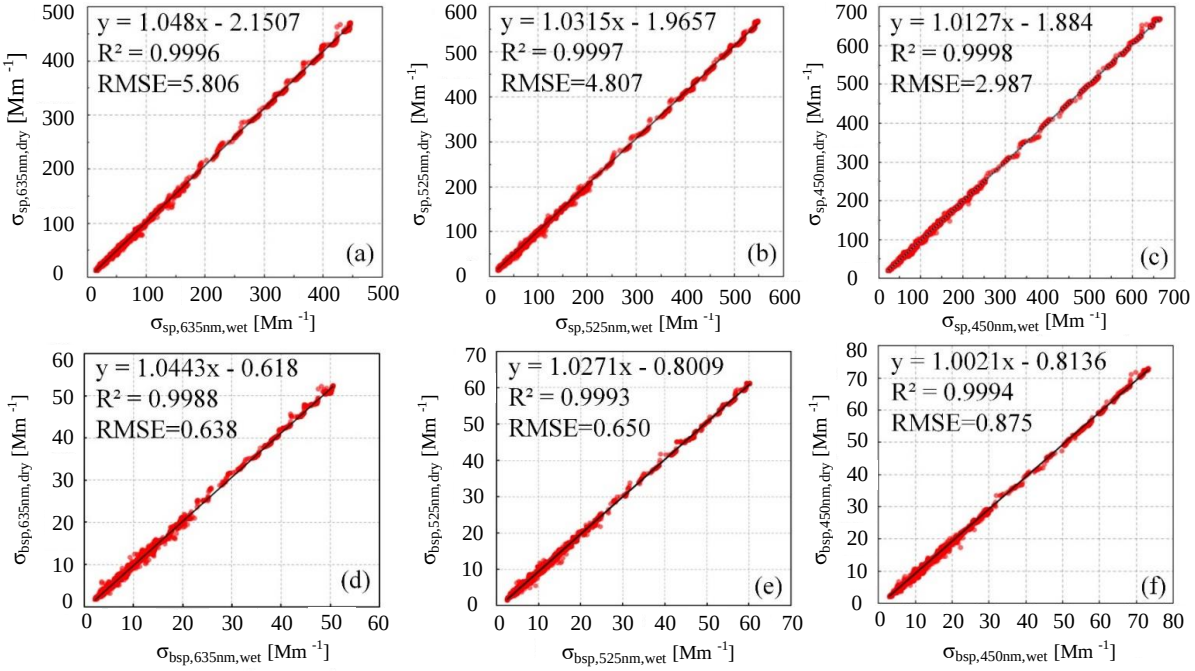

Figure S1: Checking the consistency of the two nephelometers: (a) scattering coefficient at 635 nm, (b) scattering coefficient at 525 nm, (c) scattering coefficient at 450 nm, (d) back-scattering coefficient at 635 nm, (e) back-scattering coefficient at 525 nm, and (f) back-scattering coefficient at 450 nm measured by the two nephelometers. The linear regression function, coefficient of

determination (R^2), and root-mean-square error (RMSE) are given in the upper-left corner of each panel.

With increasing wavelength, both the mean value and the standard deviation of *f*(RH = 85%) increase slightly. The hygroscopic enhancement factor is wavelength dependent, a property useful for estimating aerosol radiative forcing. Figure S2 shows the histogram for *f*(RH = 85%, 525 nm) overlaid with the Gaussian-fit curve (in green). Also shown are two other Gaussian-fit curves, i.e., for *f*(RH = 85%, 450 nm) and *f*(RH = 85%, 635 nm).

Table S1: Statistical values of *f*(RH = 85%) at 450, 525, and 635 nm (STD: standard deviation; prctl: percentile; N: sample size).

λ	mean	STD	90th prctl	75th prctl	median	25th prctl	10th prctl	N
450 nm	1.57	0.10	1.66	1.64	1.59	1.52	1.41	294
525 nm	1.64	0.13	1.75	1.72	1.67	1.59	1.44	294
635 nm	1.70	0.15	1.84	1.79	1.74	1.65	1.46	294

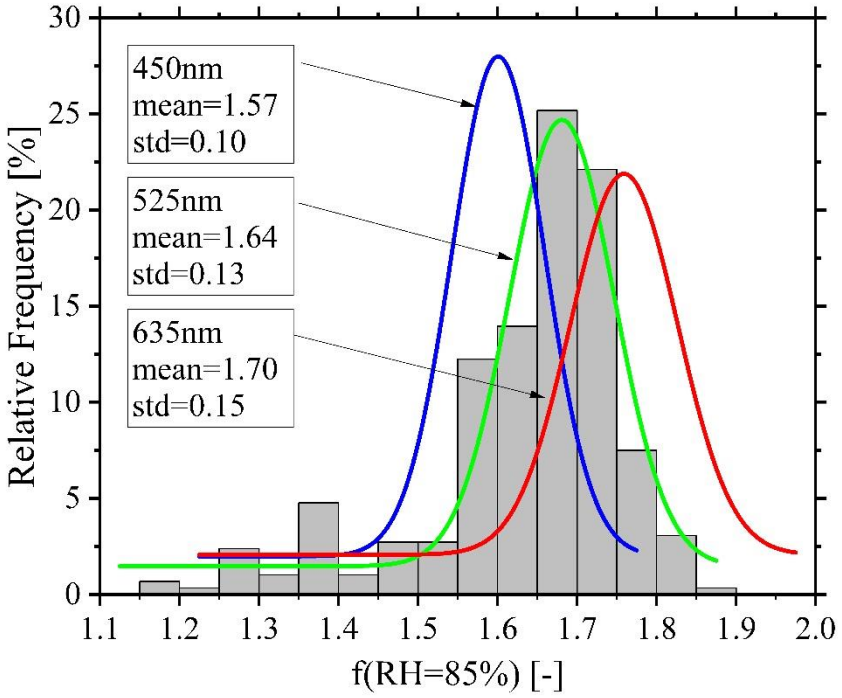

Figure S2: Frequency distribution histogram of *f*(RH = 85%, 525 nm) overlaid with Gaussian fitting curves based on statistical analyses of *f*(RH = 85%, 450 nm), *f*(RH = 85%, 525 nm), and *f*(RH = 85%, 635 nm), represented by blue, green, and red curves, respectively.

Figure S3 shows the sum of non-refractory submicron aerosol (NR-$PM_{2.5}$) mass concentrations (i.e., organics + sulfate + nitrate + ammonium + chloride) observed by the ACSM and BC mass concentrations measured by the AE33 (red curve), referred to as NR-BC-$PM_{2.5}$. Also shown are $PM_{2.5}$ mass concentrations measured by the Tapered Element Oscillating Microbalance (TEOM) at Yizhuang (blue curve). Both trends agree well, with a correlation coefficient (R) equal to 0.94 (Fig. S4). However, there are times when the $PM_{2.5}$ mass concentrations measured by the TEOM are greater than NR-BC-$PM_{2.5}$.

The main reason is that even though the BC mass concentration is considered, the ACSM does not measure refractory components like crustal material. Another reason may be that the TEOM-measured $PM_{2.5}$ mass concentrations were made at another location, so was not sampling the same air.

Figure S3: Time series of NR-BC-$PM_{2.5}$ mass concentrations measured by the ACSM and AE33 (red curve) and $PM_{2.5}$ mass concentrations measured by the TEOM (blue curve).

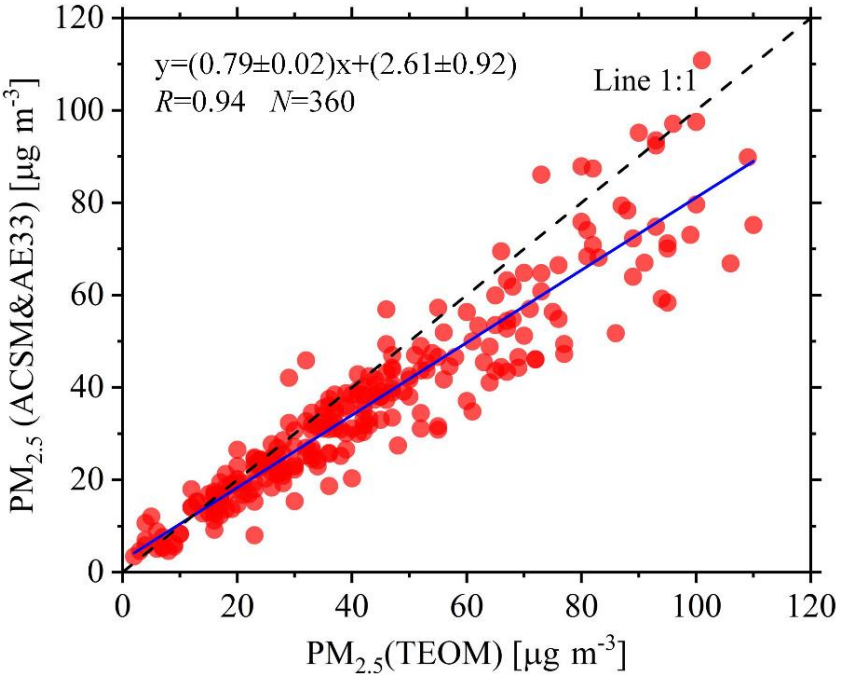

Figure S4: NR-BC-$PM_{2.5}$ measured by the ACSM and the AE33 as a function of $PM_{2.5}$ measured by the TEOM.

Aerosol acidity is one of the most important factors affecting the hygroscopicity of aerosols. The pH of ambient aerosols is estimated by comparing the mass concentration of NH_4^+ and $NH_{4\,\mathrm{predicted}}^+$, which is the amount of ammonium needed to thoroughly neutralize chloride, nitrate, and sulfate ions (Y. Sun et al., 2012):

$$NH_{4\,\mathrm{predicted}}^+ = 18 \times \left(2 \times \frac{SO_4^{2-}}{96} + \frac{NO_3^-}{62} + \frac{Cl^-}{35.5}\right). \quad (1)$$

Figure S5 shows NH_4^+ as a function of $NH_{4\,\mathrm{predicted}}^+$. The regression slope is 0.845±0.004, which is slightly less than 1. This implies that the ambient NH_3 was not sufficient to neutralize HCl, HNO_3, and H_2SO_4. $PM_{2.5}$ aerosols at the observatory in suburban Beijing were thus faintly acidic during the observation period, benefitting the hygroscopic enhancement of ambient aerosols.

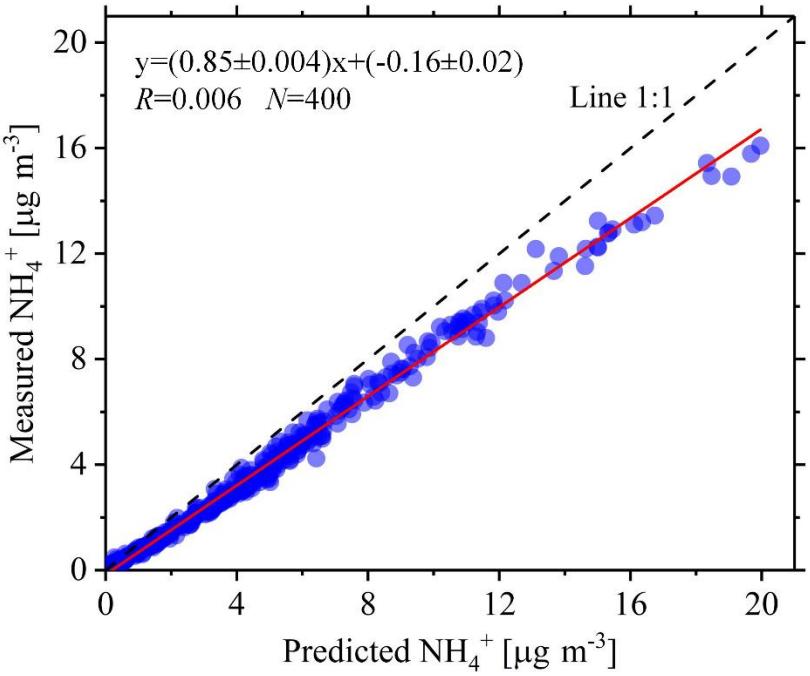

Figure S5: Measured ammonium concentration as a function of predicted ammonium calculated using Eq. (1).

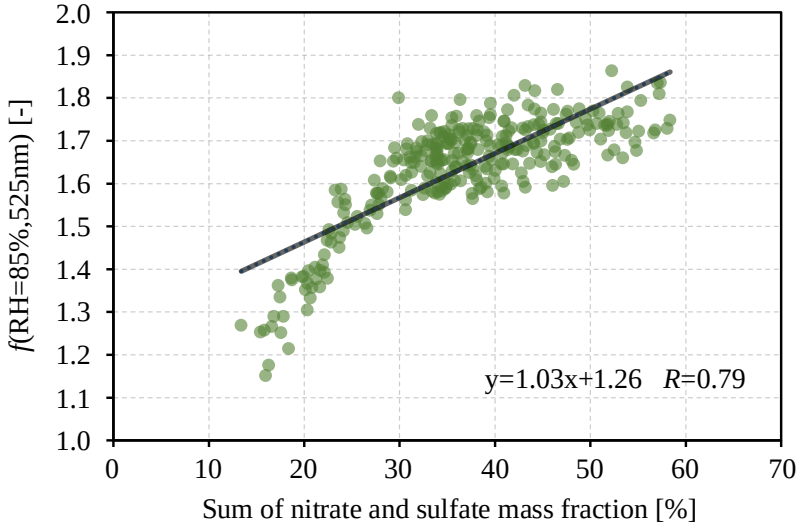

Figure S6: Hygroscopic enhancement factor *f*(RH = 85%, 525 nm) as a function of the sum of nitrate and sulfate mass fractions.

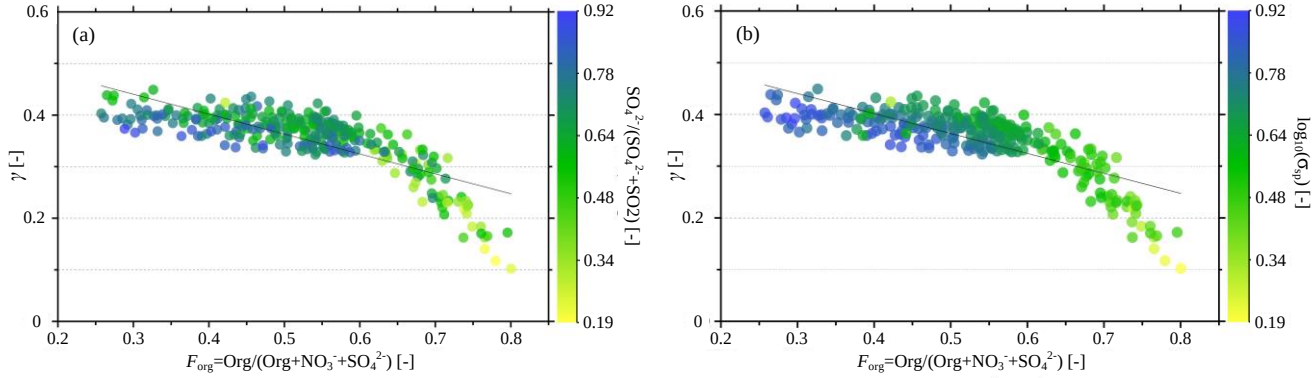

Figure S7: γ as a function of F_{org}=Org/(Org+NO_3^- + SO_4^{2-}), colored by (a) the $SO_4^{2-}/(SO_4^{2-}+SO_2)$ molar ratio and (b) $log_{10}(\sigma_{sp})$.

Figure S8 shows that the deliquescence RH of the pure ammonium sulfate aerosol generated in the laboratory was 80.367%, measured by our high-resolution humidified nephelometer system.

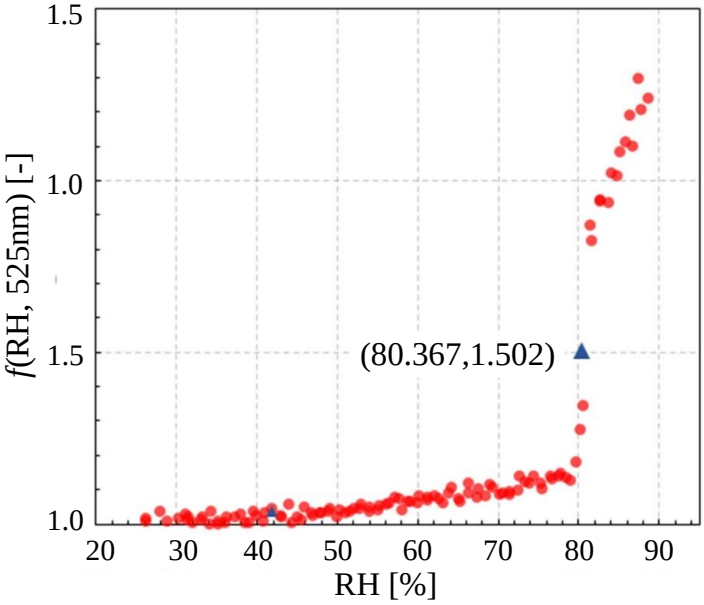

Figure S8: Deliquescence results of the pure ammonium sulfate aerosol generated in the laboratory.